A DC-link Voltage Balancing Algorithm for Three-Level Neutral Point Clamped (NPC) Traction Inverter Drive in Field Weakening Region

Abhijit Choudhury, *Student Member*, *IEEE* and Pragasen Pillay, *Fellow*, *IEEE*

Power Electronics and Energy Research (PEER) Group
P. D. Ziogas Power Electronics Laboratory
Department of Electrical and Computer Engineering
Concordia University
Montreal, Quebec H3G 1M8, Canada

***Abstract*– A DC-link voltage balancing algorithm for a three-level neutral point clamped (NPC) traction inverter drive with interior permanent magnet synchronous machine (IPMSM) is proposed. The proposed strategy is able to reduce the neutral point potential fluctuation (NPPF) considerably compared to the conventional strategy with field weakening region, when the phase current starts to lead the phase voltage. A detailed analytical study is then carried out to show the root cause of higher DC-link capacitor voltage fluctuation in the field weakening region. The proposed strategy is based on the virtual space vector, where the medium voltage vectors are used only for 1/3rd of the total duty time. In this proposed strategy the positive and negative redundant voltage vectors are used separately in a switching cycle to keep the capacitor voltage difference low, even at high load torque changes. A 6.0 kW interior PMSM is used for simulation and experimental verification. Detailed simulation and experimental studies are carried out to show the efficacy of the proposed control strategy.**

***Index Terms* – Electric vehicle, inverters, interior permanent magnet motors, propulsion, traction.**

I. INTRODUCTION

Three-level neutral-point-clamped (NPC) inverters are generally being used for medium and high power applications after its introduction in [1]. As many IGBT switches are generally connected in series depending on number of levels, they can block high DC-link voltage with reduced voltage ratings of the power switches. Due to that the switching losses also reduce compared to the conventional two-level inverter [2]. Moreover, at higher switching frequencies it is an added advantage because the three-level inverter losses will be considerably lower than the two-level inverter [3]. Hence, the cooling system will be smaller in size. For this reason electric vehicle manufacturing companies are now trying to replace the two-level with three-level inverters, so that they can operate the system at higher DC-bus voltage and switching frequencies. At higher DC-bus voltage the load current is comparatively lower for similar power level. Hence, the power switches are not restricted by the thermal limitation. However, three-level NPC inverter has a potential problem of DC-link capacitor voltage unbalance. Hence, different control strategies are proposed to reduce the neutral point potential fluctuation (NPPF).

In literature the NPPF reduction strategy is mainly classified into three categories; (a) Space vector based strategy, (b) Carrier based strategy, and (c) Virtual space vector based strategy.

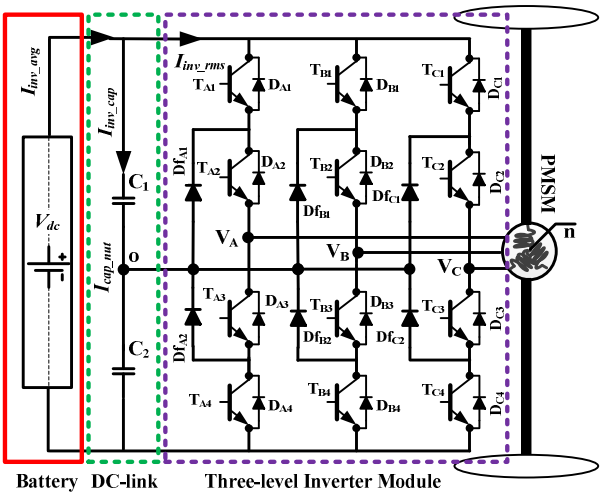

Fig. 1. Three-level neutral point clamped (NPC) traction inverter.

In [4]-[6] a space vector based NPPF reduction strategy is proposed, based on the nearest three voltage (NTV) vector. In this strategy depending on the two capacitor voltages the positive and negative redundant voltage vector time periods are changed to keep the NPPF low. However, in transients the redundancy factor (α) can go out of limit and affect the capacitor voltage balancing. For electric vehicle applications the condition is more severe because of the rapid load torque variation.

Another NTV based strategy based on redundant voltage vector sharing factor (α) is proposed in [7]-[9]. However, the switching sequences in the subsectors are different which makes asymmetric switching. To overcome this problem sub sector 1 and 2 are further subdivided into two, which makes

978-1-4673-7637-2/15/$31.00 ©2015 IEEE

the switching sequences symmetrical. However, it increases the system complexity.

To overcome the problem of online change in redundancy factor (α) and to keep the switching sequence symmetrical a novel control strategy is developed by authors in [10]. In this strategy the positive and negative redundant states are used alternatively based on the difference between the two capacitor voltages. Results showed required steady state and transient stability of the system. A modified strategy is also proposed in [11], which takes care of the lagging power factor condition to keep the NPPF low.

As the carrier based strategy reduces the computational time and complexity of the system compared to the SVPWM based strategy [12], they are also used to keep the NPPF low. A discontinuous pulse width modulation (DPWM) based strategy is proposed in [13]. In this strategy based on the difference between the two capacitor voltages, an offset voltage is generally added with the reference modulation signals. However, in transients the value of offset might go out of limit and can clamp one of the phases permanently. For electric vehicle applications the condition is even more severe because of rapid speed and torque transients.

A continuous PWM based strategy instead of DPWM as shown in the earlier reference is shown in [14]-[16]. In this strategy the difference between the two capacitor voltages are passed through a PI controller and the output from it was added with the reference modulation signals. As the PI output was directly added with the modulation signal, all the noise present in the sensed signal also appeared on the modulating signal. It contributes harmonics to the generated signal. Moreover, it also suffers from the problem of inappropriate addition of DC-offset voltage addition with the reference modulating signals. If the value of PI parameters are make low, it will increase the balancing time and will affect the system responses as shown in [17].

Hence, to keep the fast voltage balancing ability of the SVPWM strategy as proposed in [10] and to reduce the computational time of the system a hybrid PWM strategy is proposed in [18], [19]. In this strategy the duty cycles are generated based on a carrier based strategy and redundant states are identified. After that depending on the state of two capacitor voltages the positive and negative redundant states are interchanged to keep the two capacitor voltages balanced.

All the strategies proposed earlier are applicable to systems with higher power factor, where the medium voltage vectors do not influence the capacitor voltage differences significantly. However, when the system power factor reduces below a particular level or goes leading the currents start to flow through antiparallel diodes, which are uncontrollable. Hence, to reduce the influence of medium voltage vectors a virtual space vector based strategy is proposed in [20]. In this strategy the virtual vector is generated by equal sharing of the small and medium voltage vectors. As the usage of medium voltage vectors reduced to $1/3^{rd}$ in the virtual voltage vector, it also helps to reduce the NPPF. However, in the earlier proposed strategy both the positive, negative redundant states and medium voltage vectors are used with equal time sharing. This is a kind of natural balancing and the summation of three phase currents needs also to be zero. Hence, for a system with high load torque change the capacitor voltage difference might go out of limit and affect the system performance.

To overcome this problem an active virtual space vector (AVSV) based strategy is proposed in this paper for interior permanent magnet synchronous machine drives [21]. In this strategy, based on the difference between the two capacitor voltages the positive and negative redundant voltage vectors are selected to keep the neutral point balanced and the summation of the three phase currents also need not be zero.

Detailed simulation and experimental studies are carried out to show the effectiveness of the proposed system. Results showed the required performance of the system.

The paper is organised as follows: Section II gives a general over view of three-level NPC inverter, effect of medium voltage vector on NPPF, and the proposed strategy to reduce the NPPF at field weakening region for IPMSM. Simulation and experimental verification studies are demonstrated in section III and IV. It is then followed by conclusion in section V and acknowledgement in section VI.

II. PRINCIPLES OF OPERATION

A. Conventional Space Vector Based Pulse Width Modulation (VSV-PWM) for Three-level Inverter

Fig. 1 shows the general configuration of a three-level neutral point clamped traction inverter drive. Compared to the 2-level inverter the number of power electronics components are almost double and the common points of diodes are connected to the two capacitor neutral (O) points. That is where the problem of unbalanced capacitor voltages comes from. Here, I_{inv_cap} is the RMS capacitor ripple current, I_{inv_avg} is the average current supplied by battery and I_{cap_nut} is the neutral point capacitor RMS current. There are also six additional power diodes connected to the neutral point of the DC-link.

B. Virtual Space Vector Pulse Width Modulation (VSV-PWM) for Three-level Inverter

Fig. 2 shows the conventional space vector diagram used for NPC inverter in normal operation and table I shows the switching sequence for sector 1. The performance of the system is quite satisfactory when the machine operates below base speed, as already shown by authors in [10].

However, as the machines goes into the field weakening region additional –ve *d*-axis current needs to be injected to reduce the effect of the magnet flux.

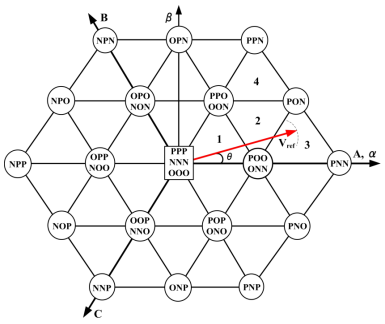

Fig. 2. Space vector diagram for three-level inverter.

Due to this –ve *d*-axis current, the resultant stator phase current (I_s) starts to go in phase with voltage (v_{ph}) and eventually goes leading, as shown in fig. 3. Here, I_s, I_{s1}, I_{s2} are the different values of phase currents with change in power factor angle, E_{ph} is the back emf, i_d, i_q are the *d-q* axis components of the phase currents and λ is the magnet flux linkage.

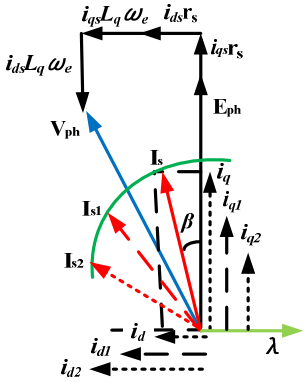

Fig 3. Phasor diagram for IPMSM.

Table I: Previously proposed DC-link voltage balancing sequence for IPMSM.

Sector	Subsector	Balancing Ability	Switching Sequence
1	1	$V_{dc1} > V_{dc2}$	OOO-POO-PPO-POO-OOO
		$V_{dc2} > V_{dc1}$	NNN-ONN-OON-ONN-NNN
	2	$V_{dc1} > V_{dc2}$	POO-PPO-PON-PPO-POO
		$V_{dc2} > V_{dc1}$	ONN-OON-PON-OON-ONN
	3	$V_{dc1} > V_{dc2}$	POO-PON-PNN-PON-POO
		$V_{dc2} > V_{dc1}$	ONN-PNN-PON-PNN-ONN
	4	$V_{dc1} > V_{dc2}$	PPO-PPN-PON-PPN-PPO
		$V_{dc2} > V_{dc1}$	OON-PON-PPN-PON-OON

C. *Effects of Leading Power Factor on NPPF*

As shown in fig. 3 with increase in negative *d*-axis current to drive the machine into deep field weakening region, the power factor improves and after a certain time it even goes leading (i_{s1}, i_{s2}). At this point when the modulation index is one (M.I. = 1.0) and the reference phase voltage is in the outer most sub-sectors (sub-sector 2, 3, 4), the redundant voltage vectors cannot control the neutral point voltage fluctuation most effectively. In this sub-sector the difference in capacitor voltages are mostly dominated by the medium voltage vectors. The situation goes worse when the phase current starts leading the phase voltage and starts to flow through the antiparallel diodes of the power switches and come back to the source side.

Fig. 4 (a), shows the simulation results for time duration for which different voltage vectors are applied (small, medium, large) and Fig. 4 (b) shows their effects on the DC-link capacitor voltage deviation, when the machine is operated at high modulation index and leading power factor angle. It can be seen that with the large voltage vectors there is no change in capacitor voltage deviation as was expected. With the redundant voltage vectors the capacitor voltage difference was trying to decrease, but due to the short time duration it was not able to make the difference zero.

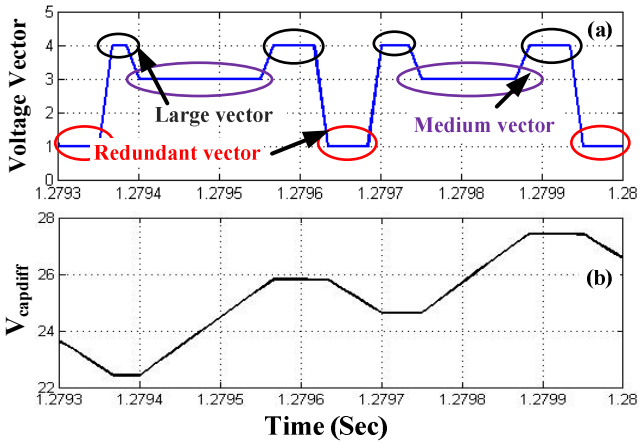

Fig. 4. Effects of different voltage vectors at higher modulation index (M ~ 1.0) and at leading power factor in subsector-3 of sector-1.

The maximum capacitor voltage deviation is contributed by the medium voltage vectors, and there is no control over the capacitor voltage difference caused by them. From the results it is obvious that the only way to remove this additional neutral point voltage fluctuation is by reducing the use of medium voltage vectors.

D. *Proposed Active Virtual Space-Vector based DC-link Voltage Balancing Strategy*

As the complete elimination of medium voltage vectors will introduce higher voltage THD at the output voltage waveforms, an active virtual space vector based strategy is introduced in this paper. The virtual vector uses both the redundant and medium voltage states equally. Due to the proposed strategy the use of medium voltage states reduce down to 1/3rd compared to the earlier proposes schemes, which helps to reduce the NPPF considerably.

Equation 1 shows the vector combination of the virtual voltage vector used for sector 1. Similar expressions can be derived for other subsectors as well. Fig. 5 shows the virtual space vector hexagon, where all the medium voltage vectors are removed by a combination of small redundant and medium voltage states.

$$V_v = (V_{PPO/OON} + V_{POO/ONN} + V_{PNO}) \cdot 1/3 \qquad (1)$$

Table II: Different vectors time periods for sectors I

Sub-Sector	T_a	T_b	T_c
1	$2M\sin(\frac{\pi}{3}-\theta)$	$1-2M\sin(\frac{\pi}{3}+\theta)$	$2M\sin(\theta)$
2	$2\{1-\sqrt{3}M\sin(\frac{\pi}{6}+\theta)\}$	$3\{2M\sin(\frac{\pi}{3}+\theta)-1\}$	$2\{1-\sqrt{3}M\cos(\theta)\}$
3	$2\{1-\sqrt{3}M\sin(\frac{\pi}{6}+\theta)\}$	$3M\sin(\theta)$	$\sqrt{3}M\cos(\theta)-1$
4	$\sqrt{3}M\sin(\frac{\pi}{6}+\theta)-1$	$3\{1-M\sin(\frac{\pi}{3}+\theta)\}$	$\sqrt{3}M\cos(\theta)-1$
5	$\sqrt{3}M\sin(\frac{\pi}{6}+\theta)-1$	$3M\sin(\frac{\pi}{3}-\theta)$	$2\{(1-\sqrt{3}M\cos(\theta)\}$

Table III: Proposed DC-link voltage balancing sequence

Sector	Sub- sector	Balancing Ability	Switching Sequence
1	1	$V_{dc1} > V_{dc2}$	OOO-POO-PPO-POO-OOO
		$V_{dc2} > V_{dc1}$	OOO-OON-ONN- OON-OOO
	2	$V_{dc1} > V_{dc2}$	POO-PPO-PNO-PPO-POO
		$V_{dc2} > V_{dc1}$	ONN-OON-PNO-OON-ONN
	3	$V_{dc1} > V_{dc2}$	POO-PPO-PNN-PNO-PNO-PNN-PPO-POO
		$V_{dc2} > V_{dc1}$	OON-ONN-PNN-PNO-PNN-ONN-OON
	4	$V_{dc1} > V_{dc2}$	PPN-PPO-POO-PNO-PNN-PNO-POO-PPO-PPN
		$V_{dc2} > V_{dc1}$	OON-ONN-PNN-PNO-PPN-PNO-PNN-ONN-OON
	5	$V_{dc1} > V_{dc2}$	PPO-POO-PNO-PPN-PNO-POO-PPO
		$V_{dc2} > V_{dc1}$	OON-ONN-PPN-PNO-PNN-ONN-OON

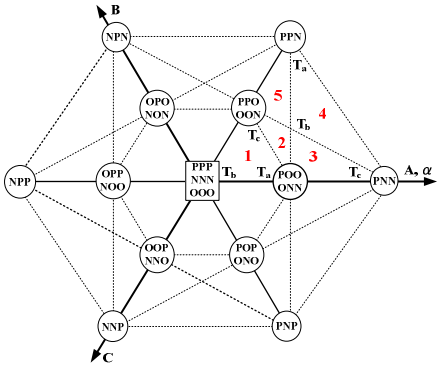

Fig. 5. Virtual space-vector diagram for the three-level inverter.

The duty cycles for all the voltage vectors are calculated by equation shown in table II. The duty time for all the voltage vectors are calculated based on the nearest three vector (NTV) strategy. The switching sequences for the proposed strategy with DC-link voltage balancing is shown in table III.

Here, modulation index (M) can be represented as $\sqrt{3}V_{ref}/V_{dc}$ and V_{dc} is the total DC-link voltage.

From table III it can be observed that all the subsectors are divided by positive and negative voltage vectors. When the upper capacitor voltage is higher than the lower one ($V_{dc1} > V_{dc2}$), the positive redundant voltage vectors are going to be used and when the lower capacitor voltage is higher than the upper on ($V_{dc2} > V_{dc1}$), the negative redundant vectors will be used in the switching sequence. Fig. 6 shows the control circuit diagram of the proposed strategy. The two capacitor voltages will be sensed and passed through a control logic block. Inside the SV-PWM control table III is implemented. Depending on the two capacitor voltages switching sequences will be selected to keep the NPPF low.

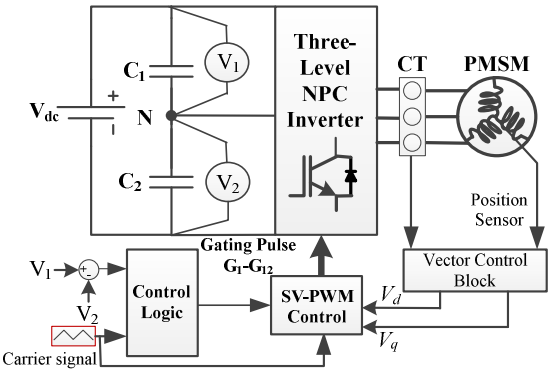

Fig. 6. NPC inverter control circuit with DC-bus voltage balancing [10].

In the earlier proposed VSV strategy [20] the virtual vector was generated by combining particular small and medium voltage vectors which can produce a summation of three-phase currents to zero. Hence, both the positive and negative redundant voltage vectors were used in one switching cycle. However, for the proposed active VSV strategy the positive and negative redundant states are used alternatively based on

the states of two capacitor voltages. It makes the balancing of the two capacitor voltages guaranteed.

III. SIMULATION STUDIES

All the simulation studies are carried out in MATLAB/Simulink platform with 270.0 V DC-bus voltage, 3.0 kHz switching frequency and 6.0 kW interior PMSM (IPMSM).

Figs. 7, 8 show the simulation results for change in machine speed from 800.0 r/min to 1200.0 r/min with the conventional and proposed control strategy. During the change in machine speed load torque was kept constant at 6.0 N.m. At 1200.0 r/min the machine goes to over modulation and to reduce the modulation index a –ve *d*-axis current of 6.0 A is injected at 3.7 sec. As a result of this the stator current increased from 2.8 A to 5.3 A. Due to the large *d*-axis current, stator current leads the phase voltage and the neutral point fluctuation goes high with the conventional strategy. This is because of the reason already explained in section II, C.

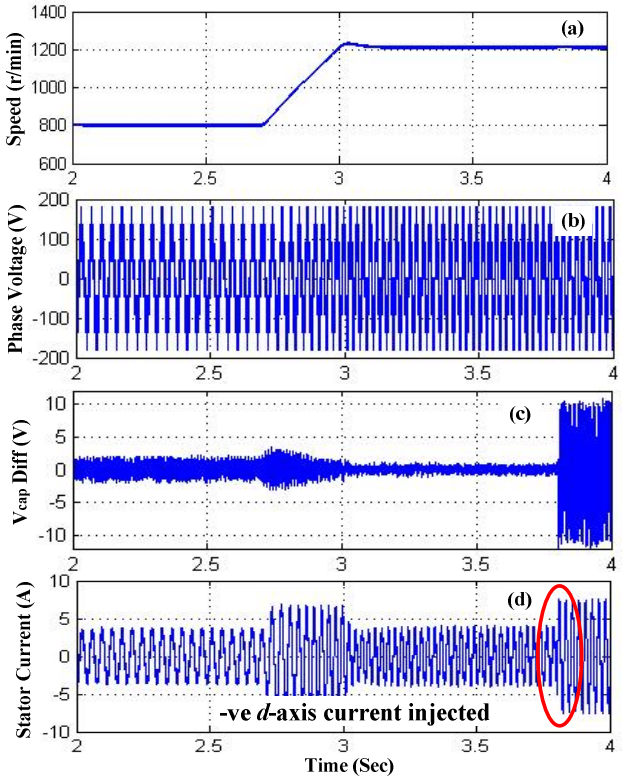

Fig. 7. Performance results for change in machine speed from 800.0 r/min to 1200.0 r/min at 6.0 N.m. load torque with the conventional strategy; (a) Change in speed; (b) Phase voltage; (c) Difference between two DC-link capacitor voltages; (d) Stator current.

However, with the proposed strategy the NPPF is quite low, as the medium voltage vectors are replaced by a virtual vector. Where with the conventional strategy the maximum capacitor voltage deviation was 20.0 V, with the proposed strategy it is 3.8 V. Hence, a total reduction of 81.0% was achievable, which is quite significant.

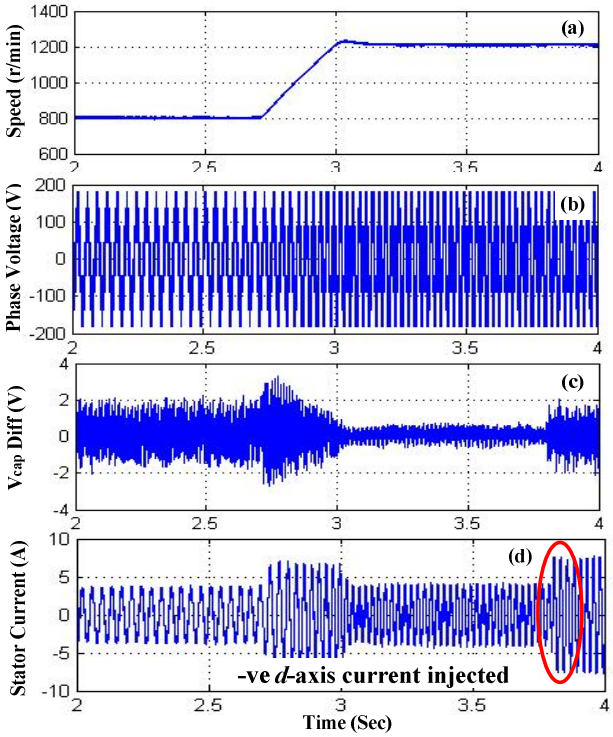

Fig. 8. Performance results for change in machine speed from 800.0 r/min to 1200.0 r/min at 6.0 N.m. load torque with the proposed strategy; (a) Change in speed; (b) Phase voltage; (c) Difference between two DC-link capacitor voltages; (d) Stator current.

IV. EXPERIMENTAL STUDIES

The proposed control algorithm is tested on a 6.0 kW interior PMSM with 6.0 N.m. load torque. Experimental work is carried out with a dspace® based real time operating system.

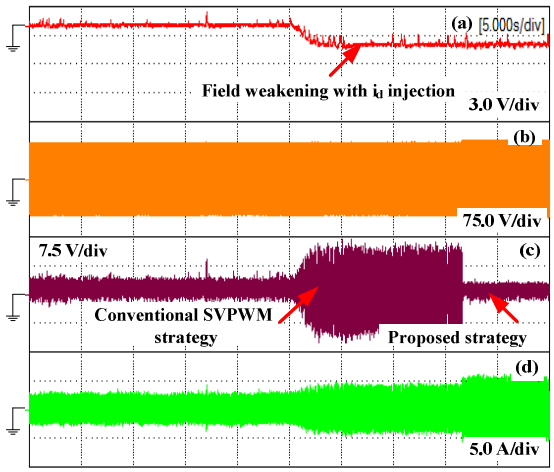

Fig. 9. Performance results for both conventional and proposed control strategy; (a) Change in *d*-axis current; (b) stator phase voltage; (c) Difference between the two DC-link capacitor voltages; (d) Stator current.

As with the previously proposed DC-link balancing scheme a lot of capacitor voltage deviation occurs at the neutral point in field weakening region, to keep the system safe the DC-link voltage was kept low at 150.0 V. The motor was run at above base speed and 2.0 A of negative *d*-axis

current was injected. From the results it can be seen that, with the conventional strategy the peak to peak capacitor voltage deviation is around 28.0 V and with the proposed control strategies it is only 4.5 V. Hence, there is a reduction of 83.9% compared to the conventional strategy.

V. CONCLUSIONS

A virtual space vector based DC-link voltage balancing strategy is developed for a three-level neutral point clamped traction inverter drive with interior permanent magnet machines in the field weakening region. As in the field weakening region the stator phase current leads the phase voltage, it creates a considerable amount of NPPF with the conventional strategy. This is because of the medium voltage vectors. The proposed control uses a virtual space vector which reduces the contribution of medium voltage vectors in the field weakening region. Both the simulation and experimental verification studies are carried out to show the effectiveness of the proposed control strategy. Results show a considerable reduction in the total neutral point capacitor voltage fluctuation with the proposed strategy.

VI. ACKNOWLEDGEMENT

This research work is done as part of NSERC/Hydro-Québec Industrial Research Chair entitled "Design and Performance of Special Electrical Machines".

VII. REFERENCES

[1] A. Nabae, I. Takahashi, and H. Akagi, "A new neutral-point-clamped PWM inverter," *IEEE Trans. on Ind. Appl.*, vol. 17, no. 5, pp. 518-523, Sept. 1981.

[2] A. Choudhury, P. Pillay, and S. S. Williamson, "Comparative analysis between two-level and three-level DC/AC electric vehicle traction inverters using a novel DC-link voltage balancing algorithm," *IEEE Journal of Emerging and Selected Topic in Power Electronics*, vol. 2, no. 3, pp. 529-540, Sept. 2014.

[3] A. Choudhury, P. Pillay, M. Amar and Sheldon. S. Williamson, "Reduced switching loss based DC-bus voltage balancing algorithm for three-level neutral point clamped (NPC) inverter for electric vehicle application," *Proc. on IEEE Energy Conversion Congress and Exposition*, Pittsburgh, USA, Sept. 2014, pp. 3767-3773.

[4] Y. Katsutoshi and M. H. Ahmet, "A novel neutral point potential stabilization technique using the information of output current polarities and voltage vector," *IEEE Trans. on Industry Applications*, vol. 38, no. 6, pp. 1572-1580, Nov. 2002.

[5] R. Maheshwari, S. M. Nielsen, and S. B. Monge, "Design of neutral-point voltage controller of a three-level NPC inverter with small DC-link capacitors," *IEEE Trans. on Industrial Electronics*, vol. 60, no. 5, pp. 1861-1871, May 2013.

[6] C. Newton and M. Sumner, "Neutral point control for multi-level inverters: theory, design and operational limitations," in *Proc. Annual Meeting of the IEEE Industry Applications Society*, New Orleans, LA, USA, Oct. 1997, pp. 1336-1343.

[7] J. Pou, R. Pindado, D. Boroyevich, and P. Rodriguez, "Evaluation of the low-frequency neutral-point voltage oscillations in the three-level inverter," *IEEE Trans. on Industrial Electronics*, vol. 52, no. 6, pp. 1582-1588, Dec. 2005.

[8] G. I. Orfanoudakis, A. Yuratich, and S. M. Sharkh, "Nearest-vector modulation strategies with minimum amplitude of low-frequency neutral-point voltage oscillations for the neutral-point-clamped converter," *IEEE Trans. on Power Electronics*, vol. 28, no. 10, pp. 4485-4499, Oct. 2013.

[9] H. Zhang, S. J. Finney, A. Massoud and B. W. Williams, "An SVM Algorithm to balance the capacitor voltages of the three-level NPC active power filter," *IEEE Trans. on Power Electronics*, vol. 23, no. 6, pp. 2694-2702, Nov. 2008.

[10] A. Choudhury, P. Pillay, and S. S. Williamson, "DC-link voltage balancing for a 3-level electric vehicle traction inverter using an innovative switching sequence control scheme," *IEEE Journal of Emerging and Selected Topic in Power Electronics*, vol. 2, no. 2, pp. 296-307, June 2014.

[11] A. Choudhury, P. Pillay and Sheldon. S. Williamson, "Modified DC-bus voltage balancing algorithm based three-level neutral point clamped PMSM drive with low power factor," in *Proc. on IEEE XXIth International Conf. on Electrical Machines (ICEM)*, Berlin, Germany, Sept. 2014, pp. 2448-2453.

[12] A. Choudhury, P. Pillay, and S. S. Williamson, "A performance comparison study of space-vector and carrier-based PWM techniques for a 3-level neutral point clamped (NPC) traction inverter drive," *in proc. on IEEE PEDES*, Mumbai, India, Dec. 2014, pp. 1-6.

[13] J. Pou, J. Zaragoza, S. Ceballos, M. Saeedifard, and D. Boroyevich, "A carrier-based PWM strategy with zero-sequence voltage injection for a three-level neutral-point-clamped converter," *IEEE Trans. on Power Electronics*, vol. 27, no. 2, pp. 642-651, Feb. 2012.

[14] P. Chaturvedi, S. Jain, and P. Agarwal, "Carrier-based neutral point potential regulator with reduced switching losses for three-level diode-clamped inverter," *IEEE Trans. on Industrial Electronics*, vol. 61, no. 2, pp. 613-624, Feb. 2014.

[15] R. Maheshwari, S. Munk-Nielsen, and S. Busquets-Monge, "Design of neutral point voltage controller of a three-level NPC inverter with small DC link capacitor," *IEEE Trans. on Ind. Electron*ics, vol. 60, no. 5, pp. 1861–1871, May 2013.

[16] A. Bendre, G. Venkataramanan, D. Rosene, and V. Srinivasan, "Modeling and design of a neutral-point voltage regulator for a three-level diode-clamped inverter using multiple-carrier modulation," *IEEE Trans. on Industrial Electronics*, vol. 53, no. 3, pp. 718-726, June. 2006.

[17] J. Jaragoza, J. Pou, S. Ceballos, E. Robles, C. Jaen, and M. Corbalan, "Voltage-balance compensator for a carrier-based modulation in the neutral-point-clamped converter," *IEEE Trans. on Industrial Electronics*, vol. 56, no. 2, pp. 305-314, Feb. 2009.

[18] A. Choudhury, P. Pillay, and Sheldon. S. Williamson, "A Hybrid-PWM Technique Based DC-Link Voltage Balancing Algorithm for a 3-Level Neutral-Point-Clamped (NPC) DC/AC Traction Inverter Drive," in *Proc. on IEEE Applied Power Electronics Conference and Exposition (APEC)*, Charlotte, NC, Mar. 2015, pp. 1347-1352.

[19] A. Choudhury, P. Pillay, and Sheldon. S. Williamson, "A Hybrid-PWM Technique Based DC-Link Voltage Balancing Algorithm for a 3-Level Neutral-Point-Clamped (NPC) DC/AC Traction Inverter Drive," *IEEE Journal of Emerging and Selected Topic in Power Electronics*, vol. pp, no. 99, pp. 1-1, 2015.

[20] S. B. Monge, J. Bordonau, D. Boroyevich, and S. Somavilla, "The nearest three virtual space vector PWM-a modulation for the comprehensive neutral point balancing in the three-level NPC inverter," *IEEE Power Electronics Letters*, vol. 2, no. 1, pp. 11-15, March 2004.

[21] A. Choudhury, P. Pillay, and S. S. Williamson, "Modified DC-bus voltage balancing algorithm based three-level neutral point clamped (NPC) IPMSM drive for electric vehicle application," in *Proc. on IEEE Industrial Electronics Society Annual Conf.*, Dallas, TX, USA, Nov. 2014, pp. 3030-3035.